

An Effective Hamiltonian Molecular Orbital-Valence Bond (MOVB) Approach for Chemical Reactions as Applied to the Nucleophilic Substitution Reaction of Hydrosulfide Ion and Chloromethane

Lingchun Song,^{*,†} Yirong Mo,^{*,‡} and Jiali Gao^{*,†}

Department of Chemistry, Digital Technology Center and Supercomputing Institute,
University of Minnesota, Minneapolis, Minnesota 55455, and Department of
Chemistry, Western Michigan University, Kalamazoo, Michigan 49008

Received October 7, 2008

Abstract: An effective Hamiltonian mixed molecular orbital and valence bond (EH-MOVB) method is described to obtain accurate potential energy surfaces for chemical reactions. Building upon previous results on the construction of diabatic and adiabatic potential surfaces using *ab initio* MOVB theory, we introduce a diabatic-coupling scaling factor to uniformly scale the *ab initio* off-diagonal matrix element H_{12} such that the computed energy of activation from the EH-MOVB method is in agreement with the target value. The scaling factor is very close to unity, resulting in minimal alteration of the potential energy surface of the original MOVB model. Furthermore, the relative energy between the reactant and product diabatic states in the EH-MOVB method can be improved to match the experimental energy of reaction. A key ingredient in the EH-MOVB theory is that the off-diagonal matrix elements are functions of all degrees of freedom of the system and the overlap matrix is explicitly evaluated. The EH-MOVB method has been applied to the nucleophilic substitution reaction between hydrosulfide and chloromethane to illustrate the methodology, and the results were matched to reproduce the results from *ab initio* valence bond self-consistent-field (VBSCF) calculations. The diabatic coupling (the off-diagonal matrix element in the generalized secular equation) has small variations along the minimum energy reaction path in the EH-MOVB model, whereas it shows a maximum value at the transition state and has nearly zero values in the regions of the ion-dipole complexes from VBSCF calculations. The difference in the diabatic coupling stabilization is attributed to the large overlap integral in the computationally efficient MOVB method.

1. Introduction

Previously, we described a mixed molecular orbital and valence bond (MOVB) theory,^{1–3} in which effective diabatic states are constructed by a block-localized wave function (BLW) method at the *ab initio* level.^{4–11} In this approach, molecular orbitals (MOs) are strictly localized within individual fragments of a molecular system according to the

specific Lewis resonance structure of the reactant or product state configuration. At the same time the block-localized MOs are delocalized within each fragment, making the MOVB method extremely efficient in comparison with *ab initio* valence bond self-consistent-field (VBSCF) methods.^{12–16} In MOVB, the localized diabatic states are coupled to result in an avoid-crossing at the transition state and the ground-state adiabatic potential energy surface.^{1–3,17} Key features of the MOVB theory include (1) that MOs within each fragment are orthogonal, which makes computation efficient, and (2) that MOs between different fragments are nonorthogonal, which retains important characteristics of valence

* Corresponding author e-mail: songx184@umn.edu (L.S.), yirong.mo@wmich.edu (Y.M), and jgao@umn.edu (J.G.).

[†] University of Minnesota.

[‡] Western Michigan University.

bond (VB) theory. In the first limiting case in which there is one fragment, MOVB reduces exactly to the Hartree–Fock theory or Kohn–Sham density functional theory. In the second limiting case in which MOs are localized on atoms, the MOVB becomes an *ab initio* VBSCF model. The MOVB method can be regarded as the simplest *ab initio* VB variant, and its computational accuracy depends on the basis functions used and the coupling between diabatic states in a specific reaction. The aim of this paper is to develop an effective Hamiltonian strategy to yield accurate results on the computed reaction barrier. We make use of the second-order nucleophilic substitution (S_N2) reaction between HS^- and CH_3Cl in the gas phase to illustrate this approach.

The most widely used empirical model in computer simulations is the empirical valence bond (EVB) approach introduced by Warshel and Weiss,¹⁸ in which the reactant and product diabatic states are represented by molecular mechanics force field. For chemical reactions, a modified Morse potential is used to describe the potential energy profile for a given bond dissociation process.¹⁹ Although multiple state configurations can be constructed, a two-state model is typically employed, representing the reactant and the product diabatic state, respectively. A key assumption of the EVB model is that the diabatic states are treated as orthogonal states, thereby, resulting in a simple secular equation independent of the overlap integral between the reactant and product wave functions.^{18,19c} This is necessary because in such an implicit model wave functions are not available. The impact of this assumption can be relieved by adjusting the off-diagonal matrix element, H_{12} , which is approximated by an exponential function or simply by a constant value, adjusted to yield the desired barrier height. Consequently, the EVB potential constructed this way can reproduce the experimental activation barrier exactly.

Recently, Hong et al.^{20a} described an interesting frozen density functional theory (FDFT) model in which the total electron density of a system is separated into fragmental densities, similar to the MOVB approach in the definition of the wave functions for the diabatic states.¹ Hong et al. defined the diabatic coupling by back calculation of the delocalized ground-state energy E_g , assuming that the overlap between the two states is zero; $H_{12} = [(E_g - H_{11})(E_g - H_{22})]^{1/2}$. The FDFT method has been applied to an S_N2 reaction and a proton transfer process in water.²⁰ In this approach, the density of a diabatic state is determined at a given configuration and kept frozen throughout the entire reaction profile.²⁰ The frozen densities are considered to be an arbitrary mathematical definition without any relationship.^{20b} Nevertheless, one notices that the adiabatic ground-state energy E_g can become higher than that of the reactant diabatic state in the FDFT model (see Figure 1 of ref 20a), which would result in an imaginary value for the diabatic coupling H_{12} . Thus, it appears to be necessary to impose certain requirements, including an approximate but explicit consideration of the overlap,²¹ when densities are separated or kept frozen. It seems that *ab initio* molecular orbital and valence bond methods described here have a unique advantage that the diabatic states are well-defined with specific physical

properties that can be related to the traditional concepts of chemical bonding.^{3,12,17}

It has been noted that the use of a constant value or a simple exponential function of one or few degrees of freedom for the off-diagonal matrix element is not flexible enough to fit both structure and vibrational frequencies at the transition state.²² To overcome this difficulty, which could be important for studying reaction dynamics including computation of kinetic isotope effects, a variety of algorithms have been proposed. Chang and Miller used a generalized Gaussian function to model the resonance integral by fitting the structure and vibrational frequencies at the transition state.²³ This approach has been extended to a multistate empirical valence bond (MS-EVB) model for modeling proton transfer reactions.^{24–26} Recently, Schlegel and co-workers further improved the Chang–Miller model by introducing a product of Gaussian and polynomial functions,^{22,27} which is aided by a remarkably efficient fitting procedure. The latter method was demonstrated to yield chemically accurate potential energy surfaces for a number of reactions. In yet another optimization approach, Truhlar and co-workers employed an interpolation scheme to reproduce the energy, gradient, and Hessian from *ab initio* methods.^{28–30}

Of course, *ab initio* valence bond (VB) theory can be directly used to construct diabatic and adiabatic states;^{12–16,31} however, there is no straightforward formulism to derive a simple two state model,^{3,32–36} representing the reactant and product diabatic states that are often used in force-field calculations. In addition, these calculations are too expensive for application to large molecules and chemical reactions in solution. Recently, we describe an approach for deriving a two-state model³ by constructing the two diabatic states from *ab initio* multiconfigurational valence bond (VBSCF) theory,^{16,37,38} and this theoretical model was used to compare results obtained from the MOVB theory.³ We showed that the effective diabatic states can be optimized by two complementary variational approaches, resulting in two limiting scenarios. In the first case, the diabatic states are constructed by optimizing the wave function of each diabatic state to yield the minimum diabatic energy; we call these states the variational diabatic configurations (VDC).^{1–3} It appears that one of the requirements for computing H_{12} in ref 21a (see eq 4 of that paper) is to obtain such states, although that approach was described in a constrained DFT model.^{21a} Alternatively, the diabatic states can be obtained as a result of the variational optimization of the valence bond wave function of the adiabatic ground state. We call these diabatic states the consistent diabatic configurations (CDC).³ Comparison between the MOVB results with those obtained using *ab initio* VBSCF theory for a model S_N2 reaction between ammonia and methylammonium ion shows that the two methods are in excellent accord in describing both the VDC and CDC diabatic states. However, the barrier heights for chemical reactions from MOVB calculations are typically a few kilocalories per mole higher than high-level *ab initio* results that include dynamic correlation.

In this paper, we show that the MOVB method can be constructed to yield the barrier height for a chemical reaction

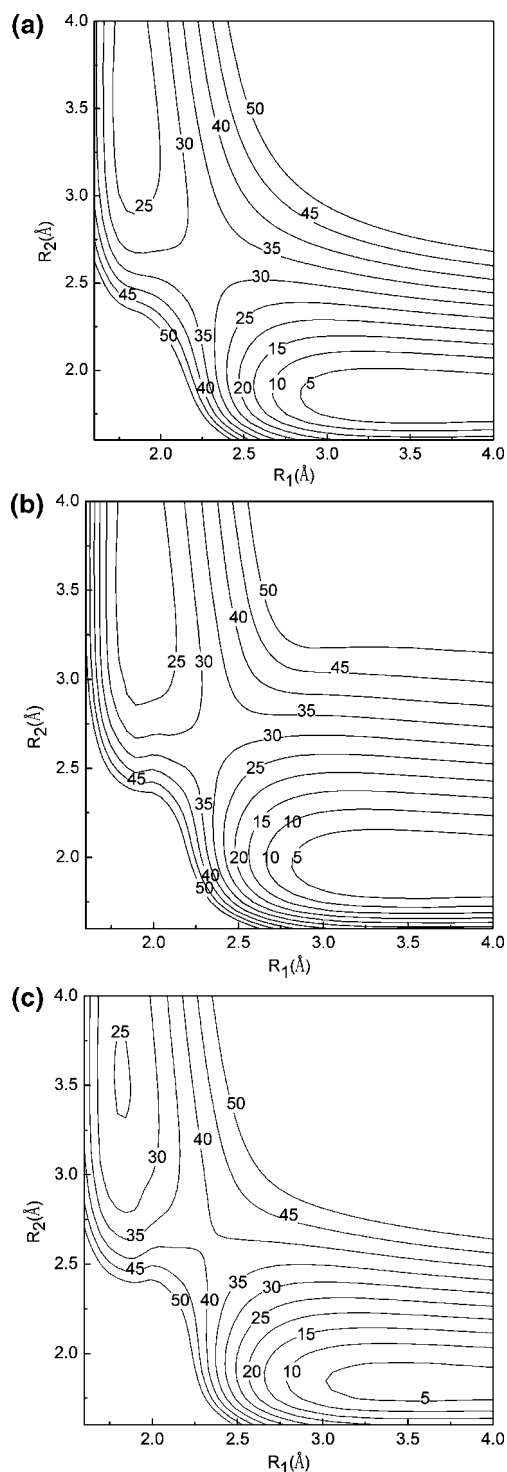
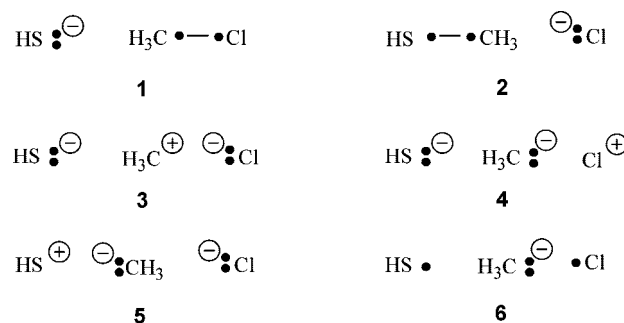


Figure 1. Computed adiabatic ground-state potential energy surface for nucleophilic substitution reaction of $\text{HS}^- + \text{CH}_3\text{Cl} \rightarrow \text{HSCH}_3 + \text{Cl}^-$ determined using (A) HF/6-31G(d), (B) VBSCF(6)/6-31G(d), and (C) CDC-MOV(2)/6-31G(d) methods. The 6-31G(d) basis set is used throughout, which will be omitted in other figures. The reaction coordinate R_1 represents the distance between the central carbon and the chlorine atom, and R_2 specifies the distance between the sulfur atom and the central carbon atom. Energies are given in kcal/mol and distances are given in angstroms. The energy of the fully separated product is chosen as the reference (zero) energy. This convention is used throughout this paper.

Scheme 1. Schematic Representation of the Valence Bond Structures for the $\text{S}_\text{N}2$ Reaction between HS^- and CH_3Cl



in exact agreement with experimental or high-level *ab initio* results. This can be accomplished by introducing a scaling factor to the exchange integral between the two diabatic states, which has minimal effects on the shape of the overall potential energy surface. We call this method the effective Hamiltonian MOV(2) (EH-MOV(2)) model. Note that the principles of constructing effective Hamiltonian valence bond theory have been used in numerous other contexts.^{22–30,39–45}

In the following, we first present the theory to systematically reduce *ab initio* valence bond configurations into a two effective state model. Then, the mixed molecular orbital and valence bond (MOV(2)) theory is reviewed, followed by a summary of computation. Results and discussions are presented next. Finally, the paper concludes with a summary of the major findings of this study and future perspectives.

2. Method

In this section, we first describe *ab initio* valence bond self-consistent-field (VBSCF) method employed in the present study as the high-level calibration target, although any other methods can be used. Then, we summarize key features of the mixed molecular orbital and valence bond (MOV(2)) theory for constructing diabatic and adiabatic potential surfaces and the effective Hamiltonian approach for obtaining accurate barrier height and energy of reaction for a chemical reaction.

A. Self-Consistent-Field Valence Bond (VBSCF)

Theory. For the $\text{S}_\text{N}2$ reaction between HS^- and H_3CCl , we consider the VB active space formed by four electrons, two from the nucleophile and two from the covalent bond between the central carbon and the leaving group chloride ion, and 3 hybridized (or polarized) atomic orbitals located on the sulfur, the central carbon, and the leaving group, respectively. Thus, a total of six VB structures can be written (Scheme 1) to form the VB wave function of the diabatic ground state. Specifically, states 1 and 2 are the covalent Heitler-London structures for the reactant and product states, respectively, each of which is represented by two Slater determinants.⁴⁶ Furthermore, each Lewis bond, the C–Cl bond in the reactant state and the S–C bond in the product state, consists of two ionic configurations, corresponding to the electron pair localized on a single atom; they are described by structures 3 and 4 and structures 3 and 5, respectively. Finally, configuration 6 represents the spin pairing interactions between an electron localized on the

nucleophilic group and one electron on the leaving group with the substrate central carbon orbital doubly occupied.

The VB wave function Φ for the S_N2 reaction between hydrosulfide ion and chloromethane is written as a linear combination of the six configurations depicted in Scheme 1.^{13,14,47}

$$\Phi = \sum_{K=1}^6 a_K \Psi_K \quad (1)$$

where Ψ_K is a Heitler-London-Slater-Pauling (HLSP) function, and a_K is the coefficient for state K . In the VBSCF theory,^{16,37,38} both the state coefficients $\{a_K\}$ in eq 1 and orbital coefficients of each VB structure $\{\Psi_K\}$ are simultaneously optimized to yield the minimum energy of the system. In this calculation, the VB atomic orbitals are the same in all configurations. The accuracy of VBSCF results is similar to that of the complete active space self-consistent field (CASSCF) method,⁴⁸ and these calculations include partial static electron correlation effects for electrons in the active space. Dynamic correlation effects can be introduced in VB calculations by relaxing the restriction on VB orbitals to allow them “breath” in different VB configurations.^{14,49–51}

B. Mixed Molecular Orbital and Valence Bond (MOVB) Theory. In the mixed molecular orbital and valence bond (MOVB) method,^{1–3,52,53} we use one Slater determinant with block-localized molecular orbitals to define individual VB configuration or Lewis resonance structure, called a diabatic state.^{4–11} The Slater determinant can be self-consistently derived at both the Hartree–Fock and DFT levels. For example, the reactant state of the S_N2 reaction between HS^- and CH_3Cl is defined as the Lewis bond structure of the substrate $\{CH_3Cl\}$ in the presence of the “spectator” nucleophilic ion $\{HS^-\}$

$$\{HS^-\}\{CH_3Cl\}; \Psi_{MOVB}^R = \hat{A}\{\chi_{HS}^R \chi_{CH_3Cl}^R\} \quad (2)$$

where Ψ_{MOVB}^R is the MOVB wave function for the reactant diabatic state, \hat{A} is an antisymmetrizing operator, and χ_{HS}^R and $\chi_{CH_3Cl}^R$ are direct products of molecular orbitals for the fragments $\{HS^-\}$ and $\{CH_3Cl\}$, respectively, constructed under the restriction that they are linear combinations of atomic orbitals located within the corresponding fragment. Furthermore, the MOs within each fragment are constrained to be orthogonal, but they are nonorthogonal between different fragments. These features are illustrated by the transformation matrix

$$C^R = \begin{pmatrix} C_{HS}^R & 0 \\ 0 & C_{CH_3Cl}^R \end{pmatrix} \quad (3)$$

where C_{HS}^R and $C_{CH_3Cl}^R$ are matrices of orbital coefficients of the occupied molecular orbitals for the two fragments.² Note that the total number of electrons within each fragment is also fixed according to the corresponding Lewis structure and there is no chemical bond between the two fragments in the present case.

Similarly, the product state is defined as the Lewis bond structure of the product $\{HSCH_3\}$ in the presence of the “spectator” ion of the leaving group $\{Cl^-\}$

$$\{HSCH_3\}\{Cl^-\}; \Psi_{MOVB}^P = \hat{A}\{\chi_{HSCH_3}^P \chi_{Cl}^P\} \quad (4)$$

where Ψ_{MOVB}^P is the MOVB wave function for the product diabatic state, and $\chi_{HSCH_3}^P$ and χ_{Cl}^P are direct products of molecular orbitals for the $\{HSCH_3\}$ and $\{Cl^-\}$ fragments, respectively.

The MOVB wave function for the adiabatic ground-state is written as a linear combination of the diabatic states

$$\Phi_{MOVB} = a^R \Psi_{MOVB}^R + a^P \Psi_{MOVB}^P \quad (5)$$

where a^R and a^P are the configurational coefficients for the reactant and product diabatic state, respectively.^{4,5} The potential energy of the adiabatic ground-state is the lower energy root of the secular equation

$$\begin{vmatrix} H_{11}^R - V & H_{12} - S_{12}V \\ H_{12} - S_{12}V & H_{22}^P - V \end{vmatrix} = 0 \quad (6)$$

where V is the adiabatic potential energy, H_{11}^R and H_{22}^P are the Hamiltonian matrix elements for the reactant and product diabatic states, respectively, H_{12} is the exchange integral, and $S_{12}^R = \langle \Psi_{MOVB}^R | \Psi_{MOVB}^P \rangle$ is the overlap integral between the two effective states.

The reactant and product diabatic states Ψ_{MOVB}^R and Ψ_{MOVB}^P can be individually optimized, giving rise to the variational diabatic configurations (VDC),^{1–3,52,53} and they can be used as basis functions to obtain the VDC-MOVB adiabatic ground-state energy with the optimization of the configurational coefficients a^R and a^P only. However, such a configuration interaction approach in the VDC-MOVB model is not a variational method. The VDC diabatic states are useful for a variety of applications; if one is interested in electronic resonance effects such as hyperconjugation stabilization of carbocations, the aromaticity of benzene and derivatives, or charge transfer effects in cation- π interactions, the VDC energies are variational for the charge localized diabatic configurations, which can be used to compare with the charge delocalized adiabatic state.^{1,2,6,9,10,54–59}

When the wave function of eq 5 is variationally optimized both in terms of the configurational coefficients a^R and a^P and in terms of the molecular orbital coefficients (eq 3) to yield the minimum energy of the adiabatic ground state, the resulting MOVB diabatic states are called the consistent diabatic configurations (CDC).³ The CDC-MOVB computational procedure is similar to that used in conventional multiconfiguration self-consistent field (MCSCF) method or *ab initio* VBSCF method, and the gradients of the adiabatic potential energy can be conveniently determined for use in geometry optimization and in molecular dynamics simulation. We note that the CDC-MOVB method is the appropriate computational approach for studying properties associated with the adiabatic ground-state such as the reaction barrier for a chemical reaction and the solvent reorganization energy. In this paper, we restrict our discussions on the CDC-MOVB method for the adiabatic ground state.

For comparison, each of the corresponding MOVB diabatic states Ψ_{MOVB}^R and Ψ_{MOVB}^P is represented by a single Slater determinant, whereas in *ab initio* VBSCF theory each state is described by three Heitler-London structures and four Slater determinants (Scheme 1). This emphasizes the com-

Table 1. Computed Binding Energies (kcal/mol) for the Formation of the Ion-Dipole (ΔE_1) Complex, the Barrier Height Relative to the IP Complex (ΔE^\ddagger), the Relative Energy between the Reactant and Product Ion-Dipole Complexes (ΔE_2), and the Net Energy of Reaction (ΔE_{rxn}) between the Product and Reactant States for the S_N2 Reaction between Hydrosulfide and Chloromethane

	HF	B3LYP	MP2	CCSD (T)	VBSCF (6) ^a	MOVB (2) ^a	EH-MOVB (2) ^a
ΔE_1	-9.3	-11.2	-9.9	-9.9	-9.9	-8.8	-10.7
ΔE^\ddagger	9.7	1.5	9.9	8.0	9.6	15.3	9.6
ΔE_2	-21.8	-18.7	-21.9	-21.5	-21.1	-22.0	-20.9
ΔE_{rxn}	-24.9	-22.3	-24.8	-24.5	-25.0	-25.0	-24.3

^a The value in parentheses is the number of structures used in the calculation.

putational efficiency of MOVB. In addition, the MOVB adiabatic ground-state defined by eq 5 does not include VB state **6** in Scheme 1, and it has been shown that exclusion of this state does not affect the energy of the adiabatic ground-state significantly in *ab initio* VBSCF calculations.³

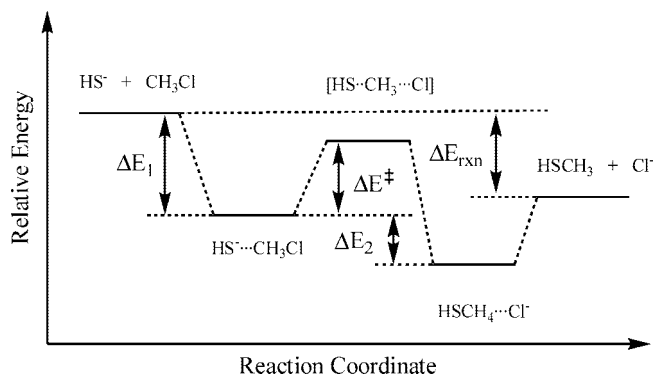
C. Effective Hamiltonian MOVB. The MOVB method has been used to study a number of nucleophilic substitution reactions and proton transfer processes both in the gas phase and in aqueous solution.^{1-3,52-54} While the overall MOVB results on diabatic states and the adiabatic ground-state are in good agreement with those obtained from *ab initio* VBSCF calculations, the computed barrier heights from MOVB are typically a few kilocalories per mole greater than high-level *ab initio* results that include electron correlations. For example, the computed barriers for the reaction of HS^- and CH_3Cl are 9.7, 9.9, 8.0, and 9.6 kcal/mol at the HF, MP2, CCSD(T), and VBSCF levels of theory using the 6-31G(d) basis set (density functional theory using the B3LYP model produces an unrealistically low barrier of 1.5 kcal/mol), but the CDC-MOVB model yields an energy barrier of 15.3 kcal/mol (Table 1). To overcome this small nagging problem in MOVB, but at the same time to retain the shape of the potential energy surface which is in accord with high-level results (Figure 1), we introduce a scaling parameter to adjust the off-diagonal Hamiltonian matrix element H_{12}

$$H_{12}^{\text{EH}} = \beta H_{12} \quad (7)$$

where H_{12}^{EH} is the effective Hamiltonian (EH) off-diagonal matrix element, and β is the diabatic coupling scaling constant to account for static correlations that are not fully accounted for in MOVB states and dynamic correlations that are not included as well as the use of a specific basis set. In such an EH-MOVB model, we retain the good qualitative and quantitative results for the diabatic states, i.e., the diagonal matrix elements H_{11}^{R} and H_{22}^{P} , in the MOVB model. We also retain the qualitative features of the off-diagonal matrix element H_{12} , but we choose a β value to reproduce exactly the barrier height of the target potential, derived either from experiment or from high-level *ab initio* calculations. In principle, the approach is similar to that used in effective Hamiltonian valence bond methods to parameterically model the *ab initio* matrix elements to reproduce the exact high-level results.^{22-30,39-45}

In addition, if the energy of reaction, which is the energy difference between the product state and the reactant state

Scheme 2. Definition and Relative Energies



from the MOVB model, is not in good agreement with experiment, we can also adjust the EH-MOVB result to match the experimental value. Here, we employ a strategy that was used in the EVB model by Warshel and co-workers by introducing a shift-parameter in the diagonal matrix element H_{22}^{P} . Let ΔE_{exp} be the experimental energy of reaction and ΔE_{MOVB} be the energy of reaction determined from the original MOVB method, which is roughly the difference between the energies of the two diabatic state, $\Delta E_{\text{MOVB}} \approx H_{22}^{\text{P}}(\mathbf{R}^{\text{P}}) - H_{11}^{\text{R}}(\mathbf{R}^{\text{R}})$, at their respective geometries \mathbf{R}^{R} and \mathbf{R}^{P} . Then, in EH-MOVB, the product state matrix element is adjusted by an energy shift-parameter $\Delta\epsilon$ as follows:

$$H_{22}^{\text{EH}} = H_{22}^{\text{P}} + \Delta\epsilon = H_{22}^{\text{P}} + (\Delta E_{\text{exp}} - \Delta E_{\text{MOVB}}) \quad (8)$$

In the EH-MOVB model, the energy of the adiabatic ground-state is determined by using the modified secular equation

$$\begin{vmatrix} H_{11}^{\text{R}} - V & \beta H_{12} - S_{12}V \\ \beta H_{12} - S_{12}V & H_{22}^{\text{P}} + \Delta\epsilon - V \end{vmatrix} = 0 \quad (9)$$

In eq 9, with the introduction of two parameters, the EH-MOVB method can be adjusted to reproduce exactly the experimental energy of activation and energy of reaction. We note that this parameter calibration approach has been used by Warshel and co-workers.¹⁸⁻²¹ The difference here is that the diabatic coupling scaling parameter uniformly modifies the entire multidimensional surface rather than a simple constant or a single-variable function.¹⁹ The value of the diabatic coupling scaling parameter is found to be in the order of 1.0005 for many reactions, and the value for the present S_N2 process is 1.00064; the value close to unity is a further indication that the shape of the potential energy surface is minimally affected, while the barrier height is reduced by about 6 kcal/mol.

3. Computational Details

All calculations are carried out using a modified version of the Xiamen Valence Bond (XMVB)¹⁶ program and Gaussian03.⁶⁰ The 6-31G(d) basis set is used throughout all calculations. Geometries for the S_N2 reaction between HS^- and CH_3Cl along the reaction coordinate defined below are optimized using the 6-31G(d) basis set at each level of theory. In VBSCF and BOVB calculations, the inner electrons are frozen at the Hartree-Fock level, and 22 valence electrons are treated in VB calculations.⁶¹

To describe the change in energy and wave function of the two Lewis bond states as the reaction takes place, we define the reaction coordinate here as the difference between the bond length of the central carbon and the leaving group $R(\text{C}-\text{Cl})$ and that of the nucleophile and the central carbon $R(\text{S}-\text{C})$:

$$R_c = R_1(\text{C}-\text{Cl}) - R_2(\text{S}-\text{C}) \quad (10)$$

Of course, one can use other definitions to monitor the progress of the reaction, including the difference between the corresponding bond orders or energies of the two Lewis bond states. The geometrical variable, corresponding to the asymmetric bond stretch coordinate, is a good choice and of chemical intuition.

4. Results and Discussion

The main goal of this study is to develop an effective Hamiltonian approach so that quantitatively accurate results can be obtained from MOVB calculations using a two-state model with a modest basis set. We aim not only to obtain accurate results for the reaction barrier and the overall energy of reaction in comparison with high-level *ab initio* results but also to ensure that the structure and the potential energy surface are adequately represented. First, we compare the adiabatic potential energy surface from *ab initio* VBSCF theory with that from MOVB calculations as a function of the bond lengths that are broken and formed in the $\text{S}_{\text{N}}2$ reaction of hydrosulfide and chloromethane. Then, we discuss the qualitative features and quantitative results for the individual diabatic configurations and the diabatic coupling integral.

A. Adiabatic Potential Energy Surface. Figure 1 illustrates the two-dimensional potential energy surfaces as functions of the $\text{S}-\text{C}$ bond length between the nucleophile and the central carbon and the $\text{C}-\text{Cl}$ distance between the central carbon and the leaving group, which are constructed by using three different levels of theory, including HF, VBSCF(6), and MOVB(2) methods, all with the 6-31G(d) basis set. The number in parentheses specifies the number of VB configurations used in the corresponding theory. In addition, the relative energies at key stationary points are summarized in Table 1 with definitions of the energy terms depicted in Scheme 2. The computational methods include the Moller–Plesset second order perturbation (MP2) theory, coupled cluster at the CCSD(T) level, and the hybrid B3LYP density function model. Overall, the results from all theoretical levels are in agreement, except for the B3LYP model which yields a surprisingly low barrier. The computed barrier heights (ΔE^\ddagger) at the transition state relative to the reactant ion-dipole complex are 9.7, 9.9, 8.0, and 9.6 kcal/mol at the HF, MP2, CCSD(T), and VBSCF(6) level of theory, respectively, and the energy differences between the two ion-dipole complexes (ΔE_2) are -21.8 , -21.9 , -21.5 , and -21.1 kcal/mol, respectively. The computed overall energies of reaction for the separated reactants and products are in good accord among these theoretical models. For comparison, the original CDC-MOVB(2) method yields a reaction barrier of 15.3 kcal/mol, an energy difference between the dipole complex of -22.0 kcal/mol, and an energy of reaction (ΔE_{rxn})

Table 2. Diabatic Coupling Scaling Parameter and the Relative Energy Shift for the Diabatic State Used in the EH-MOVB(2)/6-31+G(d,p) Method for the $\text{S}_{\text{N}}2$ Reaction between Hydrosulfide and Chloromethane^a

β (unitless)	$\Delta\epsilon$ (kcal/mol)
1.00064	0.0

^a Energies are given in kcal/mol.

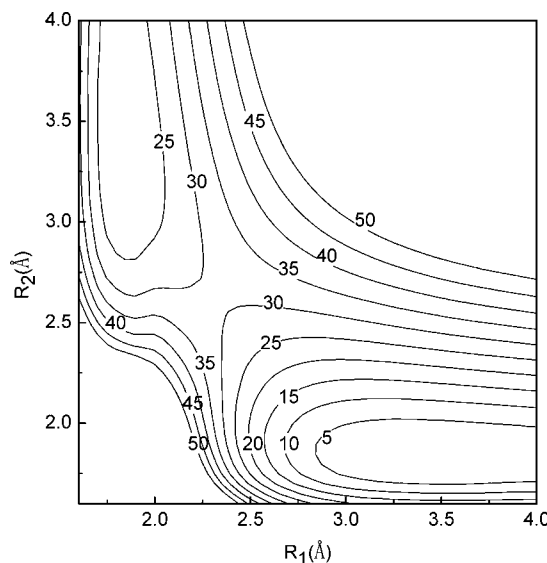


Figure 2. Adiabatic ground-state potential energy surface computed using the EH-MOVB model for the reaction of $\text{HS}^- + \text{CH}_3\text{Cl} \rightarrow \text{HSCH}_3 + \text{Cl}^-$.

of -5.9 kcal/mol. Thus, the overall performance of the MOVB(2) method is good in comparison with VBSCF results; however, the reaction barrier is overestimated by 5.7 kcal/mol relative to that of VBSCF(6) calculations. Comparison of the energy contours in Figure 1 shows that the qualitative features of the two-state MOVB(2) model are also in good accord with those obtained from HF and VBSCF(6) optimizations. This suggests that the original MOVB(2) model only needs to be slightly adjusted by lowering the barrier height by 5.7 kcal/mol but, at the same time, retaining the general qualitative features of the potential energy surface. This can be achieved within the effective Hamiltonian framework, and we have optimized the diabatic-coupling scaling parameter β in the EH-MOVB model to yield the result from *ab initio* VBSCF(6) theory. Since the relative energies between the ion-dipole complexes and the separated reactants and products are already in good accord with the VBSCF(6) values, we have decided to use an energy leveling correction of zero for the present system. The parameters in the EH-MOVB model are listed in Table 2, and the final EH-MOVB(2) results are given in Table 1. As can be seen, the exchange integral is only scaled by a factor of 0.06% of the original values.

The EH-MOVB potential energy surface for the reaction of HS^- and CH_3Cl is depicted in Figure 2, which may be compared with the *ab initio* valence bond results in Figure 1b. The original MOVB surface shows somewhat narrower contours about the minima for the two ion-dipole complexes than the VBSCF results. On the other hand, the energy contours determined using the EH-MOVB method are found

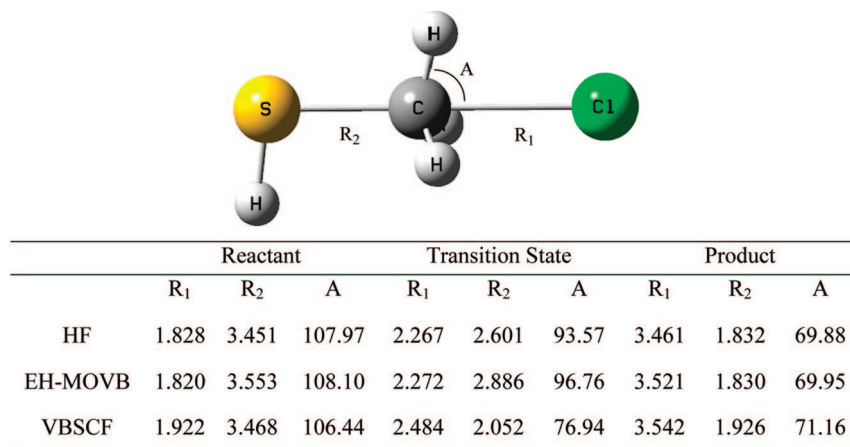


Figure 3. Key geometrical parameters for the reactant-state ion-dipole complex, the transition state, and the product ion-dipole complex optimized at the HF, EH-MOVB, and VBSCF levels of theory.

to be in good accord with the VBSCF(6) results (Figure 1b). Key geometrical parameters for the optimized transition state using different methods are shown in Figure 3. Specifically the S–C and C–Cl distances are 2.05 and 2.48 Å from VBSCF(6) theory and are 2.89 and 2.27 Å from EH-MOVB(2) optimizations. While VBSCF and EH-MOVB show large difference in the S–C bond length, the agreement between HF and EH-MOVB is reasonable. The bond angles for the hydrogen atoms that are inverted in configuration show similar trends among these three methods (Figure 3).

The energy contours for the reactant and product diabatic states are shown in Figures 4 and 5. Clearly, the shapes of these potential energy surfaces are in good agreement between the EH-MOVB and VBSCF models, although the energy contours for product diabatic state from VBSCF(6) calculations appear to be somewhat more tightly grouped. It is interesting to notice that the minimum energy paths along the coordinate of the nucleophile approaching the substrate from the upper left corner in Figures 4a and 5a mirror nicely with that of the adiabatic potential energy surface, but it deviates markedly beyond the transition state region. Of course, the energy path on the product side is more appropriately described by the product diabatic state, and it is illustrated in Figures 4b and 5b. The diabatic states are coupled, and the resulting resonance stabilization energy, also called diabatic coupling, to lower the energy of the diabatic states to yield the adiabatic potential energy surface can be defined by

$$B(\mathbf{R}) = H_{12}^{\text{EH}}(\mathbf{R}) - S_{12}(\mathbf{R})V(\mathbf{R}) \quad (11)$$

where \mathbf{R} specifies the coordinates of all atoms in the system, $V(\mathbf{R})$ is the potential energy surface of the adiabatic ground state, $H_{12}^{\text{EH}}(\mathbf{R})$ is the effective Hamiltonian off-diagonal matrix element, and $S_{12}(\mathbf{R})$ is the overlap matrix.

Shown in Figure 6 are the contour maps for the diabatic coupling both from the VBSCF(6) and the EH-MOVB(2) method. Inspecting the two diabatic coupling maps, one immediately notices that they are qualitatively different despite the fact that the potential surfaces for the adiabatic states are very similar (Figures 1b and 2). In the EH-MOVB(2) model, the energy contours for the diabatic coupling follow roughly in the direction parallel to the

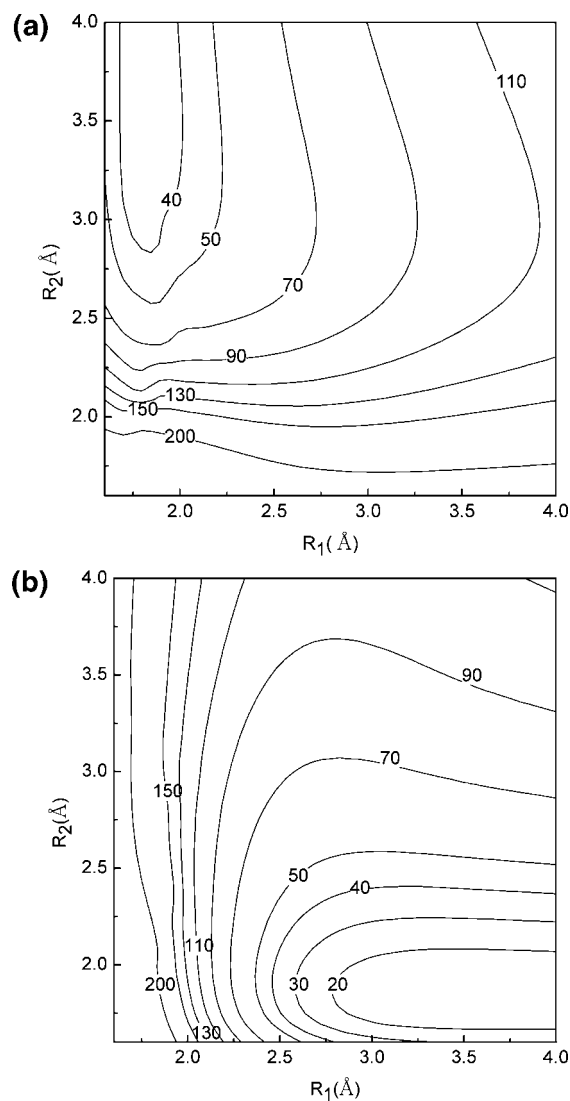


Figure 4. EH-MOVB consistent diabatic configurations for the reactant (a) and product (b) state. Energies are given in kcal/mol.

minimum energy path (MEP) of the adiabatic potential energy surface (Figure 2), whereas, in VBSCF theory, the isoenergy contour curves trace nearly perpendicularly to the MEP path. Thus, the diabatic coupling in the EH-MOVB

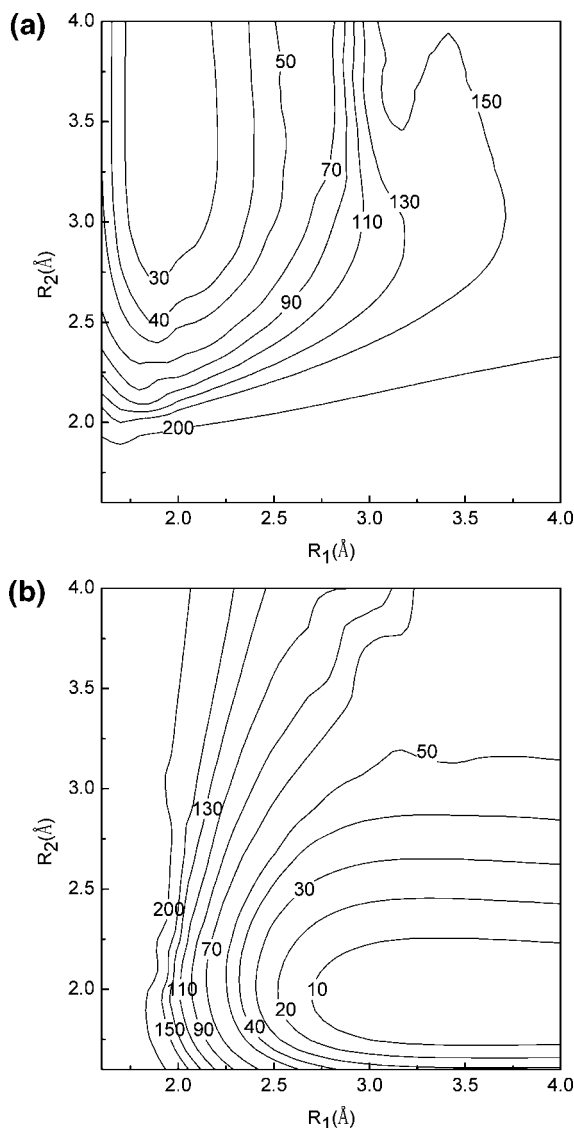


Figure 5. VBSCF consistent diabatic configurations for the reactant (a) and product (b) state. Energies are given in kcal/mol.

model has rather small variations along the MEP path coordinate, but the VBSCF diabatic coupling has a maximum at the transition state and is nearly zero at the reactant and product state (Figure 7). The difference is due to the relatively large contributions from the same ionic configuration (State 3 in Scheme 1) both in the reactant and product diabatic states in the MOVb method, resulting in greater overlap between the two states along the entire reaction coordinate. Consequently, the diabatic coupling (eq 10) shows small changes. On the other hand the overlap integral shows greater variation with geometry changes in VBSCF theory, and this dependence can be modeled by an exponential function along the MEP coordinate. Obviously, this exponential dependence is different away from the MEP, and the diabatic coupling is in general a function of all atomic coordinates (eq 10), rather than a single reaction coordinate. Interestingly, both a constant value and an exponential function have been used to mimic the diabatic coupling in applications of the EVB model.^{18,19}

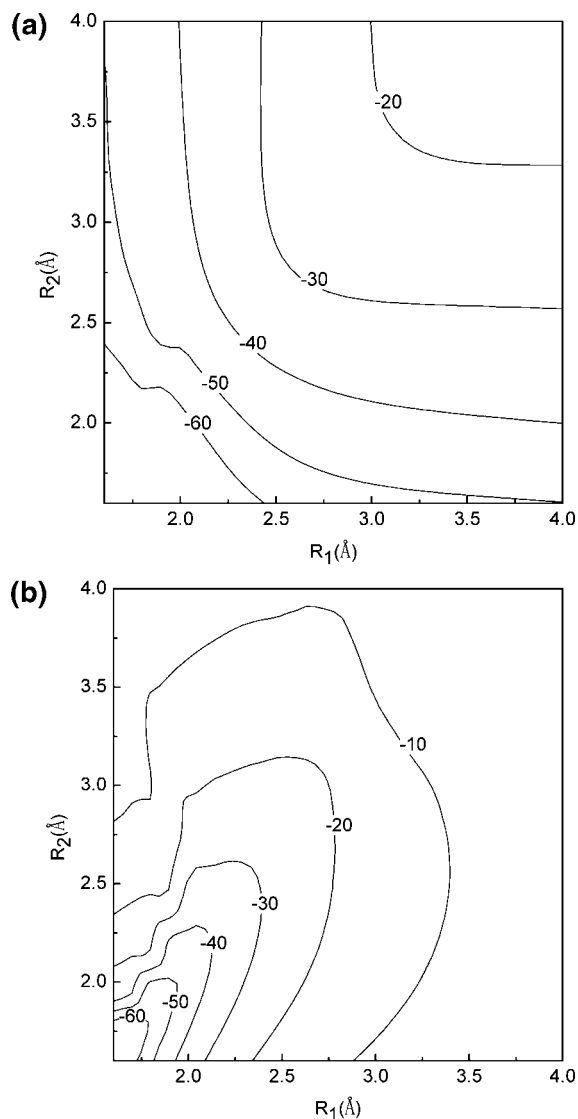


Figure 6. Computed resonance energy also called diabatic coupling (kcal/mol) for the S_N2 reaction of hydrosulfide and chloromethane using (a) the CDC-MOVb method and (b) the CDC-VBSCF approach.

B. Variational Diabatic States. The diabatic potential energy surfaces for the reactant and product states can be obtained in two different ways.³ When the diabatic states are generated as a result of variational minimization of the energy of the adiabatic ground state, they are consistent diabatic configurations (CDC).³ Alternatively, the energy of each individual diabatic state can be variationally minimized, and such variational diabatic configurations (VDC) represent the potential energy surfaces of the diabatic states ($\epsilon_1 = H_{11}$, $\epsilon_2 = H_{22}$),¹⁻³ which should be distinguished from the diagonal matrix elements (H_{11} , H_{22}) from the CDC states. This distinction is important because if one uses molecular fragments as models to parametrize the potential energy functions for the diabatic states, they correspond to the minimum energy of these states, ϵ_1 , and ϵ_2 , and thus, they are the VDC states.³

Previously, we have shown that for the S_N2 reaction between ammonia and methylammonium ion in the gas phase, the CDC states remain roughly on the covalent potential energy surface as the molecular geometry distorts

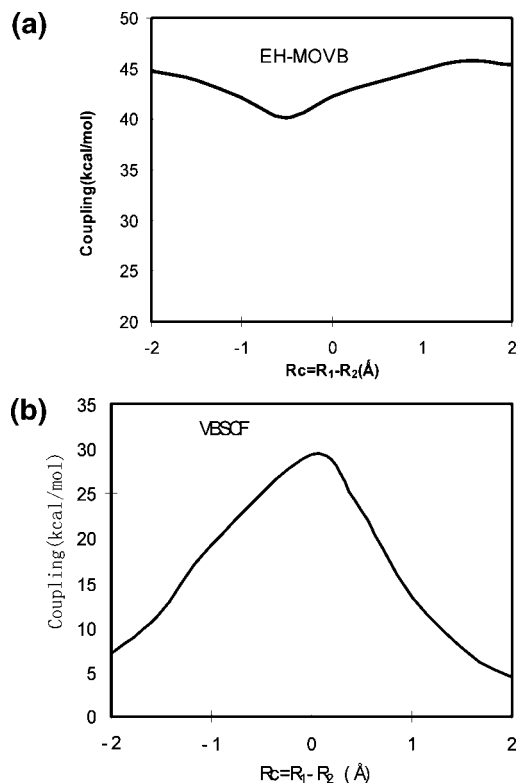


Figure 7. Computed resonance energy (kcal/mol), also called diabatic coupling, along the minimum energy path expressed by the difference between the distance between the breaking and forming bonds, i.e., $R_c = R_1 - R_2$, which is given in angstroms: (a) determined using the CDC-MOV method and (b) computed using the CDC-VBSCF model.

away from the respective reactant and product state minimum.³ On the other hand, the VDC states converge largely to the corresponding ionic configurations, which have much lower energies than the covalent states, by the same geometrical variations. These findings are clearly reflected by comparing the CDC diabatic states shown in Figures 4 and 5 with the VDC states shown in Figures 8 and 9. At the VBSCF(6) level of theory, the CDC potential surfaces (Figure 4) have energy variations of more than 200 kcal/mol both for the reactant and product states as the two chemical bonds formed and broken, respectively. On the other hand, the VDC potentials surfaces have smaller energy changes, about 130 kcal/mol within the same structural variations (Figure 8). Similar trends are observed for the EH-MOV(2) model in Figures 5 and 9, although a small subtle difference between VBSCF(6) and EH-MOV(2) can be noticed in the CDC states in that the former model seems to generate slightly less steep potential surfaces than the latter. The agreement between the VDC surfaces obtained from the VBSCF(6) and EH-MOV(2) methods is very good.

We emphasize that there is no unique way of defining the diabatic states in a two-state model to represent an intrinsically multiconfigurational wave function for the reaction system and that we have presented two approaches here to optimize the wave functions of these diabatic states. Thus, it is important to specify the way in which the diabatic states are defined and the procedure by which their wave functions are optimized to interpret the properties and reactivity of a

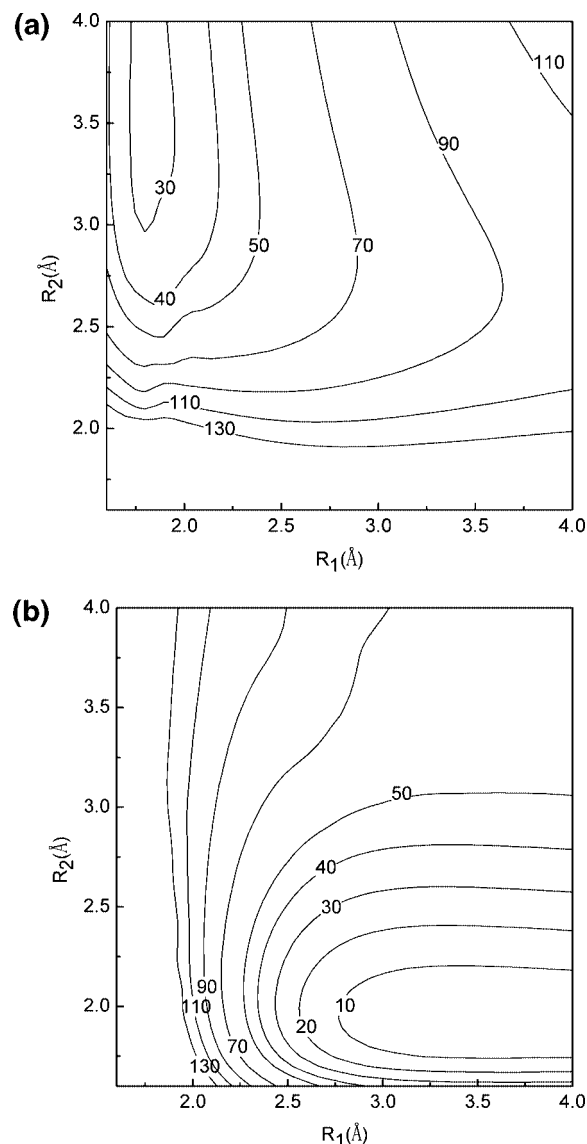


Figure 8. MOVb variational diabatic configurations (VDC) for (a) the reactant state and (b) the product state for the S_N2 reaction between hydrosulfide ion and chloromethane in the gas phase. Relative energies are given in kcal/mol.

chemical system. In addition, the nature of the diabatic states in their covalent and ionic characters will also be altered by solvation. This will significantly affect the quantitative values and the interpretation of solvent reorganization energies since the computational results depend on the charge polarization of the diabatic states. Clearly, a rigorous assessment of the definition of the diabatic states and the method used to estimate the solvent reorganization energy is as critical as the quantitative result itself.

We also note that it is sometimes informative to use a generalized solvent reaction coordinate such as the energy gap between the reactant and product diabatic states,^{1,2,19,20} $\Delta E = \varepsilon_2(\mathbf{R}) - \varepsilon_1(\mathbf{R})$. Since the energies of the diabatic states include both the internal energy change as well as the interactions with the solvent and protein media, the change in this energy difference reflects both the progress of the geometries of the reacting molecules and the polarization of the environment. This approach which was originally used in the Marcus theory for electron transfer reactions has been

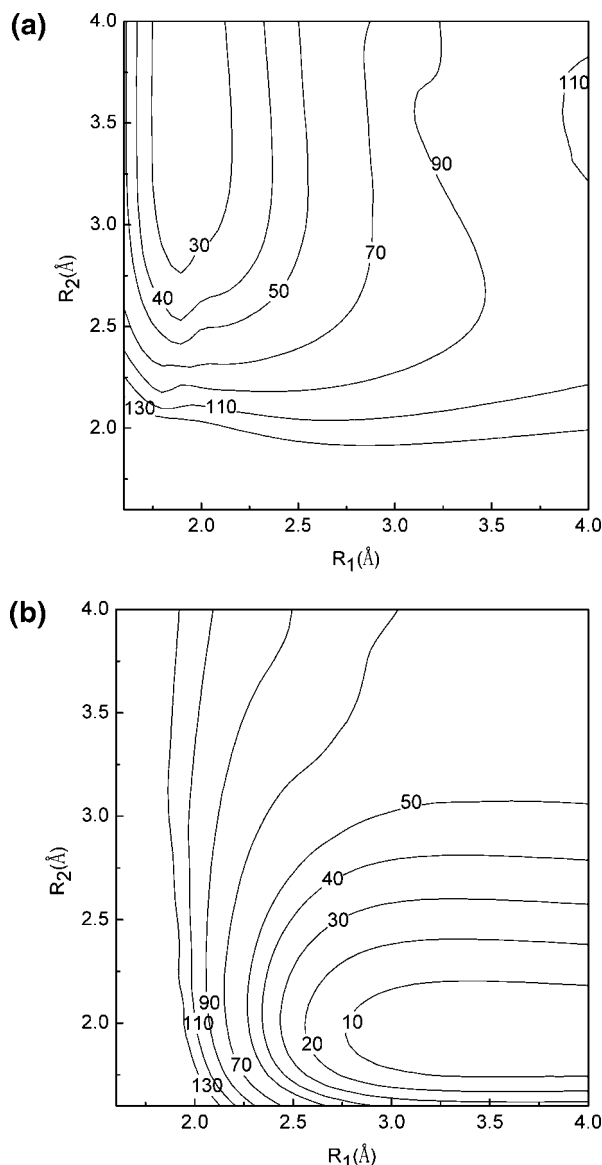


Figure 9. VBSCF variational diabatic configurations (VDC) for (a) the reactant state and (b) the product state for the S_N2 reaction between hydrosulfide ion and chloromethane in the gas phase. Relative energies are given in kcal/mol.

broadly applied, due to Warshel's work, to other chemical reactions in solution and in enzymes.^{1,2,19,20,52} In principle, the energy gap reaction coordinate can also be defined either by using the CDC states or by using the VDC states. It is straightforward computationally to employ the VDC energy gap,^{1,2,19,20} $\Delta E^{\text{VDC}} = \varepsilon_2(\mathbf{R}) - \varepsilon_1(\mathbf{R})$, as the potential energy function to directly carry out molecular dynamics simulations to obtain the potential of mean force as a function of ΔE^{VDC} for a chemical reaction.⁵² It is also desirable conceptually to use this representation since the VDC states represent the true energies of the diabatic states.

5. Conclusions

An effective Hamiltonian-mixed molecular orbital and valence bond (EH-MOVb) method has been presented to obtain an accurate potential energy surface for chemical reactions. Building upon previous results on the construction of diabatic and adiabatic potential surfaces using *ab initio*

MOVb theory,³ we introduced a diabatic coupling scaling factor to uniformly scale the *ab initio* off-diagonal matrix element H_{12} such that the computed energy of activation from the EH-MOVb method is adjusted to be in exact agreement with the target value, either directly from experiment or from high-level *ab initio* calculations. In practice, the scaling constant is only a fraction of one percent of the original value of the off-diagonal matrix element, resulting in minimal alteration of the shape of the potential energy surface of the original MOVb model. Furthermore, the relative energy between the reactant and product diabatic states in the EH-MOVb method can be improved by adding a constant value, which is the deviation from the experimental result, to the potential energy surface of the diagonal matrix element. This approach is similar to the calibration procedure used by Warshel and co-workers in the empirical valence bond (EVB) model,¹⁹ but the present EH-MOVb method is based on *ab initio* electronic structure theory in which the off-diagonal matrix elements are functions of all degrees of freedom of the system and the overlap matrix is explicitly evaluated.

We have chosen the nucleophilic substitution reaction between hydrosulfide and chloromethane to illustrate the present effective Hamiltonian approach. We used the results from *ab initio* self-consistent valence bond (VBSCF) calculations as the calibration target, noting that any other high-level methods or experimental data can be used. For the construction of diabatic states, two optimization schemes are considered. In the first approach, called consistent diabatic configurations (CDC), the wave functions for the diabatic states are obtained as a result of the variational minimization of the adiabatic ground state. In the second model, called variational diabatic configurations (VDC), the wave functions of these states are individually minimized to obtain the energy of the diabatic states. The potential energy surface for the adiabatic ground-state has been constructed using the CDC states in the two-state EH-MOVb model, and the resulting energy contours as functions of the breaking and forming bond distances are in excellent accord with those from VBSCF calculations. It was found that the stabilization energy due to diabatic coupling (the off-diagonal matrix element in the generalized secular equation) has small variations along the minimum reaction path coordinate in the EH-MOVb model, whereas it shows a maximum value at the transition state and has nearly zero values in the regions of the ion-dipole complexes from VBSCF calculations. The difference in the diabatic coupling stabilization between the two method is attributed to the large overlap integral in the computationally efficient MOVb method, which has larger contributions from the ionic state due to the use block-localized orbitals in a single determinant representation, whereas in VBSCF the overlap integral is more geometrical dependent. We have also discussed the distinction between VDC and CDC diabatic states, with the former representing the potential energy surface of the diabatic states and the latter specifying purely the diagonal matrix elements of the Hamiltonian. These differences make it necessary to clearly define the diabatic states and validate the energies in discussion of reactivity and reorganization energies.

Acknowledgment. We thank the National Institutes of Health (GM46736) and the Office of Naval Research for support of this work.

References

- (1) Mo, Y.; Gao, J. *J. Comput. Chem.* **2000**, *21*, 1458.
- (2) Mo, Y.; Gao, J. *J. Phys. Chem. A* **2000**, *104*, 3012.
- (3) Song, L.; Gao, J. *J. Phys. Chem. A* **2008**, ASAP.
- (4) Mo, Y.; Peyerimhoff, S. D. *J. Chem. Phys.* **1998**, *109*, 1687.
- (5) Mo, Y.; Zhang, Y.; Gao, J. *J. Am. Chem. Soc.* **1999**, *121*, 5737.
- (6) Mo, Y.; Gao, J.; Peyerimhoff, S. D. *J. Chem. Phys.* **2000**, *112*, 5530.
- (7) (a) Gianinetti, E.; Raimondi, M.; Tornaghi, E. *Int. J. Quantum Chem.* **1996**, *60*, 157. (b) Gianinetti, E.; Vandoni, I.; Famulari, A.; Raimondi, M. *Adv. Quantum Chem.* **1998**, *31*, 251.
- (8) Raimondi, M.; Famulari, A.; Specchio, R.; Sironi, M.; Moroni, F.; Gianinetti, E. *THEOCHEM* **2001**, *573*, 25.
- (9) Khaliullin, R. Z.; Head-Gordon, M.; Bell, A. T. *J. Chem. Phys.* **2006**, *124*, 204105/1.
- (10) Khaliullin, R. Z.; Cobar, E. A.; Lochan, R. C.; Bell, A. T.; Head-Gordon, M. *J. Phys. Chem. A* **2007**, *111*, 8753.
- (11) Mo, Y.; Song, L.; Lin, Y. *J. Phys. Chem. A* **2007**, *111*, 8291.
- (12) *Valence Bond Theory*; Cooper, D. L., Ed.; Elsevier: Amsterdam, 2002.
- (13) Cooper, D. L.; Gerratt, J.; Raimondi, M. *Adv. Chem. Phys.* **1987**, *69*, 319.
- (14) Hiberty, P. C.; Flament, J. P.; Noizet, E. *Chem. Phys. Lett.* **1992**, *189*, 259.
- (15) Wu, W.; Song, L.; Cao, Z.; Zhang, Q.; Shaik, S. *J. Phys. Chem. A* **2002**, *106*, 2721.
- (16) Song, L.; Mo, Y.; Zhang, Q.; Wu, W. *J. Comput. Chem.* **2005**, *26*, 514.
- (17) Shaik, S.; Shurki, A. *Angew. Chem., Int. Ed.* **1999**, *38*, 587.
- (18) Warshel, A.; Weiss, R. M. *J. Am. Chem. Soc.* **1980**, *102*, 6218.
- (19) (a) Warshel, A. *Computer Modeling of Chemical Reactions in Enzymes and Solutions*; Wiley: New York, 1991. (b) Aqvist, J.; Warshel, A. *Chem. Rev.* **1993**, *93*, 2523. (c) Villa, J.; Warshel, A. *J. Phys. Chem. B* **2001**, *105*, 7887.
- (20) (a) Hong, G.; Rosta, E.; Warshel, A. *J. Phys. Chem. B* **2006**, *110*, 19570–19574. (b) Xiang, Y.; Warshel, A. *J. Phys. Chem. B* **2008**, *112*, 1007–1015.
- (21) (a) Wu, Q.; Cheng, C.-L.; Van Voorhis, T. *J. Chem. Phys.* **2007**, *127*, 16419. (b) Sharir-Ivry, A.; Shurki, A. *J. Phys. Chem. A* **2008**, ASAP.
- (22) Schlegel, H. B.; Sonnenberg, J. L. *J. Chem. Theory Comput.* **2006**, *2*, 905.
- (23) Chang, Y. T.; Miller, W. H. *J. Phys. Chem.* **1990**, *94*, 5884.
- (24) Schmitt, U. W.; Voth, G. A. *J. Phys. Chem. B* **1998**, *102*, 5547.
- (25) (a) Day, T. J. F.; Soudackov, A. V.; Cuma, M.; Schmitt, U. W.; Voth, G. A. *J. Chem. Phys.* **2002**, *117*, 5839. (b) Maupin, C. M.; Wong, K. F.; Soudackov, A. V.; Kim, S.; Voth, G. A. *J. Phys. Chem. A* **2006**, *110*, 631.
- (26) Vuilleumier, R.; Borgis, D. *J. Phys. Chem. B* **1998**, *102*, 4261.
- (27) Sonnenberg, J. L.; Schlegel, H. B. *Mol. Phys.* **2007**, *105*, 2719.
- (28) Kim, Y.; Corchado, J. C.; Villa, J.; Xing, J.; Truhlar, D. G. *J. Chem. Phys.* **2000**, *112*, 2718.
- (29) Tishchenko, O.; Truhlar, D. G. *J. Phys. Chem. A* **2006**, *110*, 13530.
- (30) Lin, H.; Zhao, Y.; Tishchenko, O.; Truhlar, D. G. *J. Chem. Theory Comput.* **2006**, *2*, 1237.
- (31) Goddard, W. A., III.; Dunning, T. H., Jr.; Hunt, W. J.; Hay, P. J. *Acc. Chem. Res.* **1973**, *6*, 368.
- (32) Mead, C. A.; Truhlar, D. G. *J. Chem. Phys.* **1982**, *77*, 6090.
- (33) Pacher, T.; Cederbaum, L. S.; Koppel, H. *J. Chem. Phys.* **1988**, *89*, 7367.
- (34) Mo, Y.; Wu, W.; Zhang, Q. *J. Chem. Phys.* **2003**, *119*, 6448.
- (35) Mo, Y. *J. Chem. Phys.* **2007**, *126*, 224104.
- (36) Sidis, V. *Adv. Chem. Phys.* **1992**, *82*, 73.
- (37) Van Lenthe, J. H.; Verbeek, J.; Pulay, P. *Mol. Phys.* **1991**, *73*, 1159.
- (38) Van Lenthe, J. H.; Dijkstra, F.; Havenith, R. W. A. *Theor. Comput. Chem.* **2002**, *10*, 79.
- (39) Sheppard, M. G.; Freed, K. F. *J. Chem. Phys.* **1981**, *75*, 4507.
- (40) Hurtubise, V.; Freed, K. F. *Adv. Chem. Phys.* **1993**, *83*, 465.
- (41) Martin, C. H.; Graham, R. L.; Freed, K. F. *J. Phys. Chem.* **1994**, *98*, 3467.
- (42) Bernardi, F.; Olivucci, M.; Robb, M. A. *J. Am. Chem. Soc.* **1992**, *114*, 1606.
- (43) Bearpark, M. J.; Robb, M. A.; Bernardi, F.; Olivucci, M. *Chem. Phys. Lett.* **1994**, *217*, 513.
- (44) Bearpark, M. J.; Bernardi, F.; Olivucci, M.; Robb, M. A. *J. Phys. Chem. A* **1997**, *101*, 8395.
- (45) Bearpark, M. J.; Smith, B. R.; Bernardi, F.; Olivucci, M.; Robb, M. A. *ACS Symp. Ser.* **1998**, *712*, 148.
- (46) Heitler, W.; London, F. *Z. Phys.* **1927**, *44*, 455.
- (47) Mo, Y.; Lin, Z.; Wu, W.; Zhang, Q. *J. Phys. Chem.* **1996**, *100*, 11569.
- (48) Thorsteinsson, T.; Cooper, D. L.; Gerratt, J.; Karadakov, P. B.; Raimondi, M. *Theor. Chim. Acta* **1996**, *93*, 343.
- (49) Hiberty, P. C.; Humbel, S.; Archirel, P. *J. Phys. Chem.* **1994**, *98*, 11697.
- (50) Song, L.; Wu, W.; Hiberty, P. C.; Shaik, S. *Chem.--Eur. J.* **2006**, *12*, 7458.
- (51) Su, P.; Ying, F.; Wu, W.; Hiberty, P. C.; Shaik, S. *ChemPhysChem* **2007**, *8*, 2603.
- (52) Gao, J.; Garcia-Viloca, M.; Poulsen, T. D.; Mo, Y. *Adv. Phys. Org. Chem.* **2003**, *38*, 161.
- (53) Gao, J.; Mo, Y. *Prog. Theor. Chem. Phys.* **2000**, *5*, 247.
- (54) Mo, Y.; Gao, J. *J. Phys. Chem. A* **2001**, *105*, 6530.
- (55) Mo, Y.; Subramanian, G.; Gao, J.; Ferguson, D. M. *J. Am. Chem. Soc.* **2002**, *124*, 4832.
- (56) Mo, Y.; Wu, W.; Song, L.; Lin, M.; Zhang, Q.; Gao, J. *Angew. Chem., Int. Ed.* **2004**, *43*, 1986.
- (57) Mo, Y.; Gao, J. *Acc. Chem. Res.* **2007**, *40*, 113.
- (58) Brauer, C. S.; Craddock, M. B.; Kilian, J.; Grumstrup, E. M.; Orilall, M. C.; Mo, Y.; Gao, J.; Leopold, K. R. *J. Phys. Chem. A* **2006**, *110*, 10025.

- (59) Mo, Y.; Gao, J. *J. Phys. Chem. B* **2006**, *110*, 2976.
- (60) Frisch, M. J. G. W. T.; Schlegel, H. B.; Scuseria, G. E.; Robb, M. A.; Montgomery, J. R. C. J. A., Jr.; Vreven, T.; Kudin, K. N.; Millam, J. C. B. J. M.; Iyengar, S. S.; Tomasi, J.; Barone, V.; Cossi, B. M. M.; Scalmani, G.; Rega, N.; Petersson, G. A.; Hada, H. N. M.; Ehara, M.; Toyota, K.; Fukuda, R.; Ishida, J. H. M.; Nakajima, T.; Honda, Y.; Kitao, O.; Nakai, H.; Knox, M. K. X.; Li, J. E.; Hratchian, H. P.; Cross, J. B.; Bakken, V.; Jaramillo, C. A. J.; Gomperts, R.; Stratmann, R. E.; Yazyev, O.; Cammi, A. J. A. R.; Pomelli, C.; Ochterski, J. W.; Ayala, P. Y.; Voth, K. M. G. A.; Salvador, P.; Dannenberg, J. J.; Zakrzewski, V. G.; Daniels, S. D. A. D.; Strain, M. C.; Farkas, O.; Rabuck, D. K. M. A. D.; Raghavachari, K.; Foresman, J. B.; Cui, J. V. O. Q.; Baboul, A. G.; Clifford, S.; Cioslowski, J.; Liu, B. B. S. G.; Liashenko, A.; Piskorz, P.; Komaromi, I.; Fox, R. L. M. D. J.; Keith, T.; Al-Laham, M. A.; Peng, C. Y.; Challacombe, A. N. M.; Gill, P. M. W.; Johnson, B. W. C.; Wong, M. W.; Gonzalez, C.; Pople, J. A. *Gaussian03, Revision D.01*; Gaussian, Inc.: 2004.
- (61) Chirgwin, H. B.; Coulson, C. A. *Proc. R. Soc. London Ser. A* **1950**, *2*, 196.

CT800421Y